Environment International 127 (2019) 353–360

Contents lists available at ScienceDirect

Environment International

journal homepage: www.elsevier.com/locate/envint

Light-driven nitrous oxide production via autotrophic denitrification by self-photosensitized *Thiobacillus denitrificans*

Man Chen[a], Xiao-Fang Zhou[a], Yu-Qing Yu[a], Xing Liu[a], Raymond Jian-Xiong Zeng[a], Shun-Gui Zhou[a,*], Zhen He[b]

[a] Fujian Provincial Key Laboratory of Soil Environmental Health and Regulation, College of Resources and Environment, Fujian Agriculture and Forestry University, Fuzhou, Fujian 350002, China
[b] Department of Civil and Environmental Engineering, Virginia Polytechnic Institute and State University, Blacksburg, VA 24061, USA

ARTICLE INFO

Handling Editor: Thanh Nguyen

Keywords:
Biohybrid system
Autotrophic denitrification
Semiconductors
Cadmium sulfide
Nitrous oxide

ABSTRACT

N_2O (Nitrous oxide, a booster oxidant in rockets) has attracted increasing interest as a means of enhancing energy production, and it can be produced by nitrate (NO_3^-) reduction in NO_3^--loading wastewater. However, conventional denitrification processes are often limited by the lack of bioavailable electron donors. In this study, we innovatively propose a self-photosensitized nonphototrophic *Thiobacillus denitrificans* (*T. denitrificans*-CdS) that is capable of NO_3^- reduction and N_2O production driven by light. The system converted > 72.1 ± 1.1% of the NO_3^--N input to N_2O—N, and the ratio of N_2O-N in gaseous products was > 96.4 ± 0.4%. The relative transcript abundance of the genes encoding the denitrifying proteins in *T. denitrificans*-CdS after irradiation was significantly upregulated. The photoexcited electrons acted as the dominant electron sources for NO_3^- reduction by *T. denitrificans*-CdS. This study provides the first proof of concept for sustainable and low-cost autotrophic denitrification to generate N_2O driven by light. The findings also have strong implications for sustainable environmental management because the sunlight-triggered denitrification reaction driven by nonphototrophic microorganisms may widely occur in nature, particularly in a semiconductive mineral-enriched aqueous environment.

1. Introduction

Despite being a greenhouse gas, nitrous oxide (N_2O) is a powerful oxidant and results in a 30% increase in energy generation when 1 mol of methane is combusted with N_2O compared to oxygen (Scherson et al., 2013b). It is often used as a power booster oxidant in rockets or race cars (Scherson et al., 2013a). N_2O is produced through the thermal decomposition of ammonium nitrate at an industrial scale (Chaturvedi and Dave, 2013). N_2O is also generated as a side product of biological nitrogen removal during wastewater treatment and substantial efforts have been devoted to reducing its generation (Kampschreur et al., 2009; Santin et al., 2017). Given the great potential of N_2O in enhancing energy production, the recovery of N_2O from wastewater treatment processes has attracted increasing interest and will convert a key contaminant into a valuable resource, thereby benefitting both the environment and energy requirements (Kelly and He, 2014). This process has been achieved in a nitrogen removal process named the coupled aerobic–anoxic nitrous decomposition operation (CANDO) that resulted in the conversion of 60–65% NH_4^+-N into N_2O-N in a nitrogen-loaded wastewater (Scherson et al., 2013b).

A feasible approach for N_2O production is the reduction of nitrate (NO_3^-), one of the major nitrogenous contaminants (Ghafari et al., 2008). Such a reduction can be conducted by biological denitrification (Beaulieu et al., 2011). The accumulation of N_2O is greatly affected by the operational parameters, particularly the source and concentration of organic carbon (Adouani et al., 2010; Santin et al., 2017). However, organic carbon is often the limiting factor in a denitrification process (Shao et al., 2010). Autotrophic denitrification, which does not require an external organic carbon source, is an alternative approach for nitrate reduction and subsequent N_2O production (Van Doan et al., 2013; Zhang and Lampe, 2015). Traditional inorganic electron donors, such as reduced sulfur or hydrogen gas, are frequently used but can pose problems for autotrophic denitrification. For example, when reduced sulfur (S or FeS_2) is used to provide electrons, the sulfate (SO_4^-) product will be released to the effluent, increasing the water hardness and the potential of infrastructure corrosion (Bosch et al., 2012; Zhang and Lampe, 2015). Although hydrogen gas is a promising electron source, it has low water solubility, is difficult to transport and has a high cost

* Corresponding author.
E-mail address: sgzhou@soil.gd.cn (S.-G. Zhou).

https://doi.org/10.1016/j.envint.2019.03.045
Received 6 January 2019; Received in revised form 27 February 2019; Accepted 19 March 2019
Available online 04 April 2019

(Ghafari et al., 2008; Lee and Rittmann, 2002). Therefore, seeking an appropriate electron source is of great importance in N_2O production via autotrophic denitrification.

Solar energy is readily available and can be converted to photoelectrons via a semiconductor device. A nonphotosynthetic bacterium, *Moorella thermoacetica* precipitated with cadmium sulfide (CdS) quantum dots, is capable to selectively produce acetic acid upon irradiation (Sakimoto et al., 2016). The Wood–Ljungdahl pathway for CO_2 fixation is driven by photoexcited electrons, which are captured by membrane proteins and ultimately transported into the cytoplasm. When the gold nanoclusters were replaced with CdS as the photosensitizer, a 33% higher quantum efficiency (2.86 ± 0.38%) was obtained than the value obtained with CdS (2.14 ± 0.16%) (Zhang et al., 2018). Moreover, the addition of TiO_2 into a periphytic biofilm increases the abundance of autotrophic denitrifiers after irradiation (Zhu et al., 2018). Importantly, recent research on the interactions of microorganisms with semiconductors strongly support the possibility of photoexicted electron transfer from a semiconductor to organisms (Jiang et al., 2018; Sakimoto et al., 2016; Wei et al., 2018; Xu et al., 2018). These exciting studies inspired us to explore whether autotrophic denitrifiers also used photoexcited electrons as an electron source. Moreover, when electrons from an electrode are directly used for denitrification, N_2O readily accumulates (Van Doan et al., 2013). Here, we have developed a non-phototrophic denitrifiers photosensitized by semiconductor and investigated their abilities to reduce NO_3^- and produce N_2O without bioavailable electron donors under irradiation to verify this hypothesis. This study provides the first proof of concept evidence for sustainable and low-cost autotrophic denitrification to generate N_2O in a process driven by light. Light-driven denitrification has a potential to become a significant revolution in removing nitrogen from wastewater and recovering energy from the nitrogen.

2. Materials and methods

2.1. Construction of T. denitrificans-CdS hybrids

Thiobacillus denitrificans (DSM 12475) was purchased from the Leibniz Institute DSMZ-German Collection of Microorganisms and Cell Cultures. *T. denitrificans* was chosen as the model bacterium because it is a widely distributed and well-characterized chemolithoautotroph, that has been shown to be able to accept electrons from an electrode for denitrification (Ghafari et al., 2008; Yu et al., 2015). The inoculum was cultivated in Medium I (Table S1) at 30 °C and the cell density was monitored using a UV–Vis spectrometer (Spectronic 2000, Thermo). When the OD_{600} of medium was approximately 0.2, cysteine and Cd^{2+} were injected into the medium to final concentrations of 0.1 wt% cysteine and 1 mM Cd^{2+}. Both the cysteine and Cd^{2+} stock solutions were prepared under N_2 and sterilized before use. After 5–7 days of cultivation, the color of suspension changed from opaque white to bright yellow, indicating the formation of the *T. denitrificans*-CdS hybrid system. The suspension was centrifuged at 5000 rpm for 8 min, then washed with a 0.9% NaCl solution three times, and finally suspended to in a 20 mL Medium II in a 120 mL anaerobic bottle (Table S1), from which NH_4Cl and the electron source $Na_2S_2O_3$ were removed and the concentration of NO_3^- was reduced to 60 mg/L. This suspension was stored until irradiation.

2.2. Characterization of T. denitrificans-CdS hybrids

The UV–Vis spectra of *T. denitrificans*-CdS suspensions were recorded using a Shimadzu UV2600 spectrometer with an integrating sphere. The band gap of CdS was calculated using Tauc plots. Samples for X-ray diffusion (XRD) were washed with deionized water three times then dried at 60 °C overnight. The XRD patterns were detected using an X-ray diffractometer (XRD-6000, Shimadzu, Japan) with Cu Kα radiation at 40 kV and 30 mA and recorded in a 2θ range of 5–90° at a scan speed range of 0.2 °C/s. For the morphological observations of microorganisms, the bare *T. denitrificans* or *T. denitrificans*-CdS hybrids were fixed with 2.5% glutaraldehyde for 12 h and dehydrated with different concentrations of ethanol (50%, 75%, 90%, and 100%). The suspensions were dropped onto the silicon plate and dried at room temperature. The platinum-sputtered samples (MC1000, Hitachi, Japan) were analyzed with a field-emission scanning electron microscope (FESEM, SU8020, Hitachi, Japan). For the high-resolution analysis of morphology, the suspensions were dropped onto a carbon film, dried at room temperature, and analyzed using a field-emission transmission electron microscope (FETEM, Tecnai G2 F20 S-TWIN, FEI, USA). The composition of surface elements was analyzed using an energy dispersive X-ray detector (X-Max^N, Oxford Instrument).

2.3. Light-driven denitrification experiments

The light-driven denitrification experiments were performed under anaerobic conditions and with irradiation from an LED array composed of 395 ± 5 nm violet LEDs (3.07 ± 0.14 mW cm^{-2}) or a 300 W Xenon lamp (CEL-HXF300, Ceaulight, Beijing, China) with a 400 nm UV-cut filter. The intensities of light were measured and calibrated using a light density meter (CEL-NP2000-2, Ceaulight, Beijing, China). Because *T. denitrificans* is able to reduce NO_3^- using cysteine as an electron donor, cysteine is not a suitable sacrificial reagent in this system. Therefore, lactate was chose to act as the sacrificial reagent because it was often used in CdS based photocatalytic systems (Harada et al., 1985; Zhang et al., 2010). Prior to the experiments, 0.1% sodium lactate was added to each anaerobic bottle as the sacrificial reagent before irradiation. Each experiment was performed with three replicates.

Concentrations of NO_3^- and nitrite (NO_2^-) were determined using ion chromatography (ICS 900, Dionex, Thermo Fisher, USA). The ammonium (NH_4^+) concentration was measured using the indophenol blue colorimetry method. Prior to irradiation, the gas in the headspace was washed with high-purity helium (99.999%) and then was periodically sampled and analyzed using a robotized system, as described in a previous report (Molstad et al., 2007). Briefly, the system consisted of a gas chromatograph (GC, Agilent 7890, USA) coupled to a peristaltic pump, an autosampler and a thermostatic water bath. The concentration of N_2O in the headspace was analyzed using an Electron Capture Detector (ECD), while the concentration of N_2 and O_2 were analyzed using a Thermal Conductivity Detector (TCD). The GC condition was described in the previous report. The concentration of N_2O in the aqueous phase was measured using a previously reported method (Law et al., 2012), with some modifications. Briefly, a 1 mL sample containing N_2O was injected into a vacuum vial (120 mL) and allowed to reach liquid-gas equilibrium. The gas-phase N_2O concentration in the vial was then measured using GC, as described above, and the liquid-phase N_2O concentration was calculated based on Henry's law. The total N_2O concentration in the sample was obtained by dividing the total amount of N_2O in both the gas and liquid phases by the total liquid volume. For determination of the concentration of cadmium ions after irradiation, the 1 mL reaction solution was first filtered through a 200 nm membrane and centrifuged for 15 min at 12000 rpm. The supernatant was analyzed using inductively coupled plasma mass spectrometry (ICP-MS, NEXION 300X).

2.4. Real-time polymerase chain reaction (PCR)

After a 24 h reaction, the four samples including *T. denitrificans* (dark), *T. denitrificans* (light), *T. denitrificans*-CdS (dark) and *T. denitrificans*-CdS (light), were stored at −80 °C. Total RNAs were extracted from the four samples using a UNIQ-10 column and Trizol total RNA extraction kits. The concentration of each RNA sample was quantified with a NanoDrop2000 spectrophotometer (Thermo Scientific, U.S.). The cDNA templates were synthesized from the purified RNA using

Revert Aid Premium Reverse Transcriptase (Thermo Scientific™ EP0733). The real-time PCR assay was performed on a LightCycler 96 (Roche, U.S). Amplification reactions were performed in a volume of 20 μL and the reaction mixture contained 10 μL of 2 × SYBR® Green Real-time PCR Master Mix, 0.6 μL of each primer (Table S2), 5 μL of the cDNA templates, and 3.8 μL of RNase-free water. The thermal cycling steps for real-time PCR in all amplification reactions were: 1 cycle at 95 °C for 30 s, 40 cycles at 95 °C for 15 s, 51 °C for 60 s and 1 cycles at 95 °C for 15 s, 51 °C for 60 s, and 95 °C for 1 s (for dissociation curve). In all experiments, three replicate amplifications were performed.

2.5. Light-driven N_2O production using ^{15}N-labeled $K^{15}NO_3$ as the electron acceptor

^{15}N-labeled $K^{15}NO_3$ was used as the electron acceptor to validate the conversion of NO_3^--N to N_2O—N. After a 68 h irradiation, the gas in headspace was measured using a gas chromatography-mass spectrometer (GC-MS, 7890-5975c, Agilent, USA) in selected ion monitoring (SIM) (m/z = 31 and 46) mode.

2.6. Calculation of the quantum yield (QE)

The instant QE was calculated based on the results of first 2 h of irradiation with a 395 nm LED lamp (P_{light} = 3.07 ± 0.14 mW cm^{-2}) and the area of irradiation was 37.5 cm^2 (A). The quantum efficiency (QE) was calculated using the following equation:

$$QE = \frac{\text{the number of eletrons accepted by } NO_3^-}{\text{the number of incident photons}} \times 100\% = \frac{[2 \times C(NO_2^-) + 3 \times C(NO) + 2 \times 4 \times C(N_2O) + 2 \times 5 \times C(N_2) + 8 \times C(NH_4^+)] \times 6.02 \times 10^{23}}{\frac{P_{light} A t \lambda}{hc}} \times 100\%$$

3. Results and discussion

3.1. Construction of the T. denitrificans-CdS hybrid

CdS-photosensitized *T. denitrificans* (*T. denitrificans*-CdS) was produced using the microbial induced semiconductor precipitating process (note: CdS did not form in the absence of microorganisms). In this process, cysteine as a sulfur source and Cd^{2+} were added to the medium of a *T. denitrificans* culture in the logarithmic phase (OD_{600}~0.2) (Fig. S1). Once the medium color changed to bright yellow (Fig. S2), scanning electron microscopy (SEM) of bacterial samples was performed and the images showed a gelatinous shell covering the cells, resulting in a rough surface of *T. denitrificans* (Fig. S3a and b). Transmission electron microscopy (TEM) images clearly revealed that particles distributed on the surface of bacteria cells, and the diameters of those particles ranged from 10 to 100 nm (Fig. 1a and b). Energy dispersive X-ray spectroscopy (EDS) mapping revealed that the particles were composed of sulfur and cadmium (Fig. 1c–f). According to the powder X-ray diffusion (XRD) pattern and high-resolution TEM images, CdS was in the hexagonal phase (Fig. S4a and b). Due to the irregular shape and inhomogeneous contrast, these particles were likely clusters of smaller particles. The broad peaks in the XRD pattern (Fig. S4a) and slightly larger bandgap (2.54 eV, Fig. S5) also supported the finding that the observed CdS is composed of clusters with a small diameter (< 20 nm) (Sakimoto et al., 2016).

3.2. Light-driven NO_3^- reduction and N_2O production by T. denitrificans-CdS

A series of experiments in thiosulfate-free medium (Table SI, Medium II) was performed (Fig. 2a) to examine the feasibility of light-driven N_2O production via denitrification by CdS photosensitized *T. denitrificans*. The concentration of NO_3^--N in the *T. denitrificans* only suspension was stable at ~14 mg/L, indicating that *T. denitrificans* was unable to reduce NO_3^--N in the absence of electron donors. When *T. denitrificans* was photosensitized with CdS, complete NO_3^--N removal was accomplished after 68 h irradiation, following a first-order reaction with a kinetic constant of 0.081 ± 0.011 h^{-1} (n = 3, R^2 > 0.98). However, in the absence of light, the NO_3^--N concentration did not obviously change, suggesting a light-driven denitrification behavior of the photosensitized *T. denitrificans*. The photosensitized *T. denitrificans* suspension was autoclaved to understand the role of microorganisms in NO_3^--N reduction, and only 14.1 ± 1.5% of NO_3^--N was removed. When active *T. denitrificans* was added to the *T. denitrificans* (dead)-CdS system, the NO_3^--N removal was improved to 38.9 ± 2.8% after 68 h irradiation. The lower NO_3^--N removal efficiency observed upon re-inoculation might be related to the poor contact of newly added *T. denitrificans* with the photosensitizer CdS, thereby impeding the photoelectron transfer from CdS to *T. denitrificans* and subsequently decreasing the rate of denitrification. Those results strongly support a denitrification role for *T. denitrificans* in the *T. denitrificans*-CdS hybrids following irradiation. The optimized rate of nitrate reduction by *T. denitrificans*-CdS was achieved after irradiation with 80 mW cm^{-2} light, with a kinetic constant of 0.54 ± 0.05 h^{-1} (n = 3, R^2 > 0.98) by varying the intensities of light (20–100 mW cm^{-2}, Xenon lamp with 400 nm UV-cut filter) (Fig. 2b). The decreased removal rate and kinetic constant under high intensity light irradiation (100 mW cm^{-2}) was likely related to the formation of a large number of oxidative holes on the cell surface to disrupt the cell membrane (Wang et al., 2017).

The nitrogenous products were monitored during NO_3^--N reduction (Fig. 2c). NO_2^- was observed as the main intermediate, as its accumulation appeared first and then eventually decreased to zero. It was found that 17.8 ± 2.5% of the NO_3^--N input was converted to NH_4^+-N after 68 h irradiation, likely due to either nonselective photocatalytic NO_3^- reduction by CdS or dissimilatory nitrite reduction to ammonium (DNRA) by microorganisms. Interestingly, 72.1 ± 1.1% of the NO_3^--N input was converted to N_2O—N, corresponding to a N_2O-N concentration of 8.7 ± 0.5 mg/L, while only 2.7 ± 0.3% of NO_3^--N was converted to N_2—N. The percentage of N_2O-N in the gaseous products (N_2O-N + N_2-N) was 96.4 ± 0.4%. Based on this finding, the N_2O reductase catalyzing the formation of N_2 from N_2O was strongly inhibited during the denitrification process by *T. denitrificans*-CdS hybrids. Even after prolonging the irradiation time to 5 days, the ratio of N_2O-N in the gaseous products did not significantly decrease. The high purity of N_2O also suggests the high specificity of biological reactions. A 7.4 ± 3.4% loss of input was observed, which might have been assimilated by the microorganisms. N_2O was not be produced without NO_3^- addition. ^{15}N-labeled $K^{15}NO_3$ was used as the electron acceptor to further confirm the source of N_2O—N. Peaks at m/z = 46 and m/z = 31 were detected, and corresponded to $^{15}N_2O$ and ^{15}NO, respectively. Those results firmly confirmed that $^{15}NO_3^-$-N was reduced to $^{15}N_2O$-N (Fig. 2d).

Fig. 3a shows the four-step microbial denitrification process of $NO_3^- \rightarrow NO_2^- \rightarrow NO \rightarrow N_2O \rightarrow N_2$, which involves corresponding enzymes nitrate reductase (Nar), nitrite reductase (Nir), nitric oxide reductase (Nor) and nitrous oxide reductase (Nos). Therefore, the denitrifying genes encoding these enzymes were evaluated using real-time polymerase chain reaction (PCR) (Shao et al., 2010). As shown in Fig. 3, the expression of the genes *nar*, *nir*, *nor* and *nos* in *T. denitrificans*-CdS (light) was upregulated 11.9 ± 1.6fold, 4.6 ± 1.1fold, 8.8 ± 1.8 fold and 6.9 ± 1.1 fold compared with the control (*T. denitrificans* in the dark), respectively. However, the expression of those genes in both *T. denitrificans* grown in the light and *T. denitrificans*-CdS grown in the dark was not significantly different from the control. This firmly proved that the *T. denitrificans* in biohybrids system contributed to denitrification under irradiation. The expression of the *nos* gene was also upregulated as there was still 2.7 ± 0.3% N_2—N produced from the NO_3^--N input in *T. denitrificans*-CdS (light) (only 0.1 ± 0.0% from

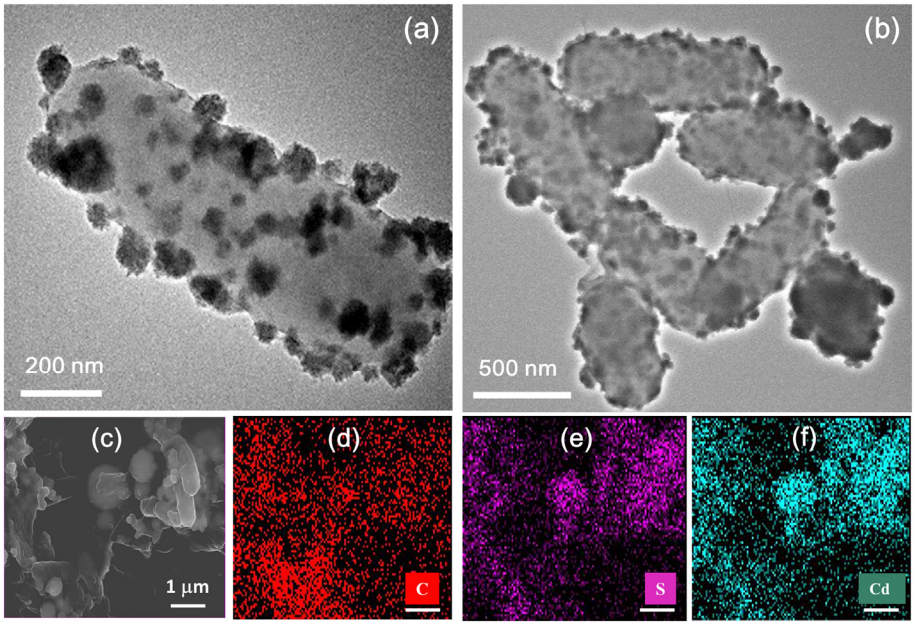

Fig. 1. Characterization of *T. denitrificans*–CdS hybrid. (a and b) TEM images of *T. denitrificans*-CdS hybrids with different scales bar of 500 nm and 200 nm, respectively. (c–f) SEM image (c) and EDS mappings shows the distribution of (d) carbon (C), (e) sulfur (S) and (f) cadmium (Cd) in *T. denitrificans*–CdS hybrids.

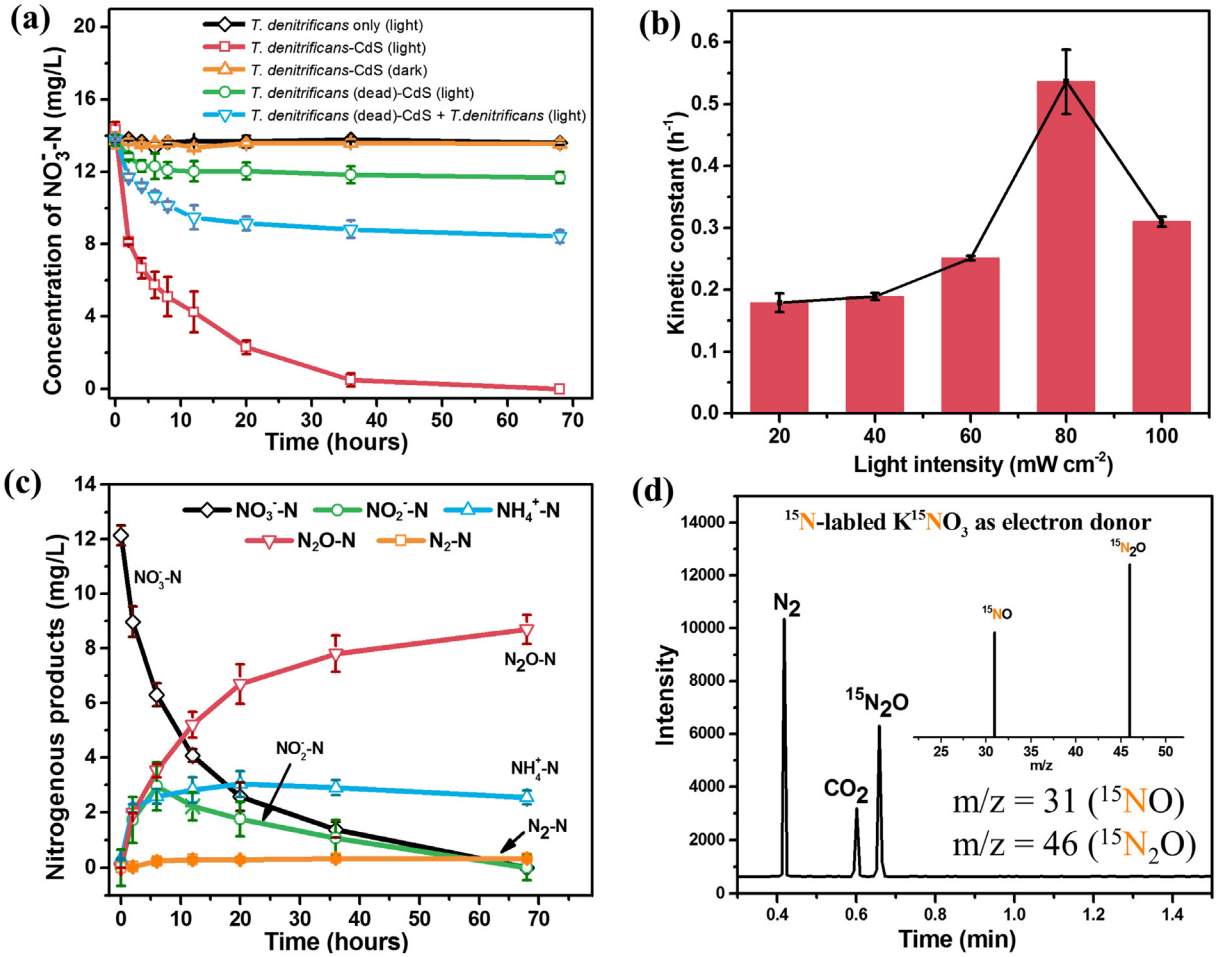

Fig. 2. Light-driven nitrate reduction by *T. denitrificans*-CdS. (a) Time curves of NO_3^--N reduction by *T. denitrificans*-CdS hybrids under 395 nm LED irradiation and control experiments. (b) Kinetic constant of nitrate reduction by *T. denitrificans*-CdS under 20–100 mW cm^{-2} of light intensities irradiation. The kinetic constants were calculated based on first-order reaction fitting. (c) Time curves of the changes of NO_3^--N, NO_2^--N, N_2O—N, N_2—N and NH_4^+-N during NO_3^--N reduction by *T. denitrificans*-CdS under 395 nm LED irradiation. (d) Gaseous products in *T. denitrificans*-CdS were detected by GC–MS after 68-h irradiation when ^{15}N-labeled $K^{15}NO_3$ was used as the electron acceptor. m/z = 31 and m/z = 46 are the peaks of ^{15}NO and $^{15}N_2O$, respectively.

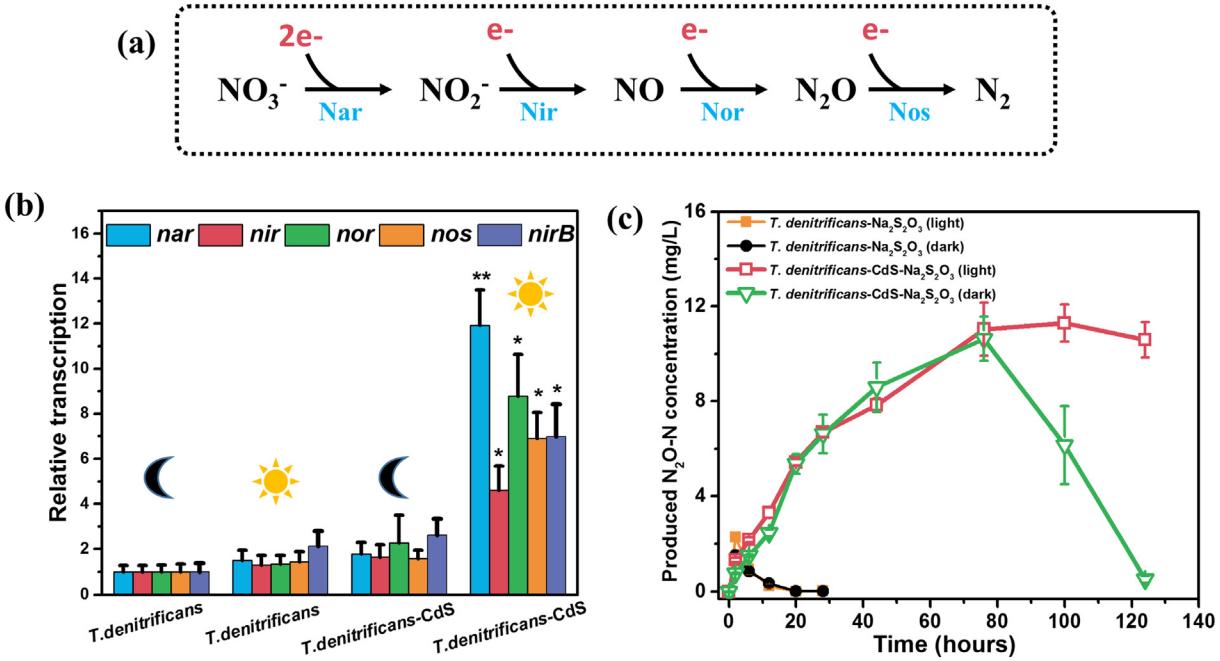

Fig. 3. Process of denitrification and genes analysis via real time PCR. (a) Process of denitrification by *T. denitrificans* and relative denitrifying proteins. (b) Relative transcript abundance of the genes (*nar*, *nir*, *nor*, *nos* and *nirB*) encoding denitrifying proteins in *T. denitrificans*-CdS and controls after 24-h reaction by real-time PCR. An asterisk (*) represents a significant difference $P < 0.05$, while two asterisks (**) represent a significant difference $P < 0.01$. (c) Time curves of N_2O-N concentration and percentages of input NO_3^--N converting to N_2O-N by *T. denitrificans* in the light (orange line) and in the dark (black line) and *T. denitrificans*-CdS hybrids in the light (red line) and in the dark (green line) when $Na_2S_2O_3$ was used as the electron sources. (For interpretation of the references to color in this figure legend, the reader is referred to the web version of this article.)

abotic reaction, shown in Table S3), indicating the Nos did not completely inhibited. Interestingly, Fig. 3b also showed the 7.0 ± 1.4fold upregulation of the expression of the *nirB* gene, which encodes the enzyme required for DNRA compared with the control, indicating that NH_4^+-N was produced through the DNRA process. Moreover, only 2.7 ± 0.3% of the nitrogenous product NH_4^+-N generated by *T. denitrificans* (dead)-CdS after 68 h, indicating that only ~15% of NH_4^+-N was produced in the abiotic reaction (Table S3). Therefore, the NH_4^+-N produced by *T. denitrificans*-CdS (light) was mainly generated in the biotic reaction.

To obtain a better understanding of N_2O accumulation via light-driven denitrification, the same concentration of *T. denitrificans*-CdS was added to a routine medium in which $Na_2S_2O_3$ was used as an electron source (Table S1, Medium I). The rates of N_2O-N production in the dark and in the light were not substantially different, indicating that irradiation did not affect the conversion of NO_3^--N to N_2O-N when an electron source other than light was available (Fig. 3c, 0➔80 h). Meanwhile, regardless of whether culture were incubated in the light or dark, N_2O-N was not significantly reduced to N_2—N at time point prior to 80 h. It might result from the sulfide generated when excess cysteine was added to form CdS in the process of bio-hybrid formation. Sulfide reacts with the redox active metal cofactor of N_2O reductase (containing a multicopper center) to form metal sulfides, and subsequent inhibit N_2O reductase (Pan et al., 2013; Richardson et al., 2009). The 5–7 times of N_2O-N accumulated by *T. denitrificans*-CdS than *T. denitrificans* alone, regardless of whether the bacteria were cultured in the light or dark, also supported that N_2O-N reduction was inhibited in the biohybrid itself (Fig. 3c). At 80 h, most of the NO_3-N input was converted to N_2O-N (~11 mg/L). A prolonged reaction (> 80 h) reduced N_2O-N to N_2—N in the dark, while the concentration of the accumulated N_2O-N did not decrease upon light irradiation (Fig. 3c, 80➔124 h). Such a difference indicates that in addition to the inhibition by bio-hybrid itself, irradiation reinforced the inhibition of N_2O reduction, resulting to the much lower N_2O-N reduction in the light than that in the dark. Because of the sensitivity of N_2O reductase to oxidative conditions, the N_2O reductase was inactivated by the formation of oxidative species (e.g., h^+, radicals) during CdS irradiation, resulting in N_2O accumulation (Alefounder and Ferguson, 1982; Bell and Ferguson, 1991; Coyle et al., 1985). To further verify this hypothesis, H_2O_2 was added to the *T. denitrificans* with NaS_2O_3 as the electron donor to determine the influence of oxidative species on N_2O-N reduction. As shown in Fig. S6, after H_2O_2 addition, higher concentration of accumulated N_2O-N and a lower rate of N_2O-N reduction were observed compared to *T. denitrificans* alone. When excess catalase was added to the *T. denitrificans*-H_2O_2 system to decompose the H_2O_2, the N_2O-N accumulation decreased to the original level. This finding supports the hypothesis that oxidative species inhibit the reduction of N_2O—N. In summary, the N_2O accumulation results from two ways: first, the N_2O reductase was inactivated by the sulfide during the formation process of *T. denitrificans*-CdS hybrids; second, the oxidative species during irradiation reinforced the inhibition of N_2O reduction. Therefore, high purity of N_2O was able to be produced in the light-driven denitrification by *T. denitrificans*-CdS.

3.3. Electron sources for denitrification by T. denitrificans-CdS under irradiation

The photocatalytic reduction by CdS and biological denitrification by *T. denitrificans* synergistically result in NO_3^- reduction. *T. denitrificans* plays the predominant role in NO_3^- reduction, because in the absence of live cells (*T. denitrificans*(dead)–CdS), only 14.1 ± 1.5% of the NO_3^--N input was removed after a 68 h reaction. By precipitating CdS nanoparticles on the bacterial cells, the transfer of photoelectrons into cells is substantially increased, thereby facilitating the denitrification process. Moreover, the bottom of the conduction band of CdS measured using the Mott-Schottky plot is −1.19 V vs. Ag/Ag/Cl (−0.99 V vs. NHE) (Fig. S7), which is thermodynamically feasible for transferring photoelectrons to the involved enzymes involved in this process, including Nar, Nir, and Nor (Eq. (2)) (Thauer et al., 1977). When *T. denitrificans*-CdS was cultured in the absence of the sacrificial

reagent, NO_3^- reduction still occurred at lower rate of nitrate reduction than in the presence of the sacrificial reagent (Fig. S8). The sacrificial reagent lactate was oxidized by the photoexcited holes and then decomposed to the corresponding oxidative products (e.g., pyruvate, CO_2, etc.) (Eq. (3)). This reaction would promote the charge separation and then enhance the transfer of the photoexcited electrons to cells (Wei-Kang et al., 2015). More economic, effective and green sacrificial reagents should be investigated in the future to improve the charge separation, enhance the rate of denitrification and reduce the cost of the system.

$$CdS \xrightarrow{h\nu} h^+ + e^- \quad (1)$$

$$NO_3^- + 2.5H_2O + 4e^- \xrightarrow[T.\ denitrificans]{Nap\ Nir\ Nor} 0.5N_2O + 5OH^- \quad (2)$$

$$Lactate + 2h^+ \rightarrow Pyruvate + 2H^+ \quad (3)$$

In a light-dark cycle experiment, the concentration of NO_3^--N decreased at a much faster rate in the light with significantly higher removal rates (3.63–8.60 $mgNO_3^-$-N L^{-1} h^{-1}) than in the dark (0.07–0.36 $mgNO_3^-$-N L^{-1} h^{-1}) (Fig. 4). NO_3^--N reduction in the dark was likely triggered by light, with some electron sources produced during irradiation. Sulfur generated by the photooxidative dissolution of CdS could serve as an electron source for *T. denitrificans*. The illumination experiment was performed in a sulfur-free medium to confirm the occurrence of sulfur-driven denitrification, (Table SI, Medium III). The concentration of SO_4^- increased from 0 to 4.9 ± 0.5 mg/L after 68 h irradiation (Fig. S9), confirming the presence of sulfur-driven denitrification ($6NO_3^- + 4S + H_2O \rightarrow 4SO_4^{2-} + 3N_2O + 2H^+$), although this pathway had a relatively minor contribution (7.7 ± 0.8%) to NO_3^--N reduction in the current system. Hydrogen (H_2) is also considered an intermediate or electron source for NO_3^- reduction in autotrophic denitrification. However, *T. denitrificans* was unable to conduct denitrification when H_2 was provided as the only electron source (Fig. S10), thereby excluding the H_2-mediated electron transfer pathway.

3.4. Proposed mechanism of light-driven denitrification

Based on the results presented above, a possible mechanism of the light-driven microbial denitrification by *T. denitrificans*-CdS hybrids was proposed (Fig. 5). When *T. denitrificans*-CdS was exposed to light, the excited photoelectrons from CdS were transferred into cells via the membrane-bound electron acceptors (e.g., quinols and C-type cytochrome) (Kornienko et al., 2016) and then to the enzymes of the denitrification pathway via a series of electron transfer chains (Chen and Strous, 2013). The close contact of CdS with bacterial cells improves the electron transfer from CdS to cells. The quantum yield (QE) in the first 2 h was 2.0 ± 0.2%, which is lower than *M. thermoacetica*-CdS but much higher than phototrophic bacteria (Larkum, 2010). The energy loss might have resulted from the recombination of e^- and h^+ or H_2 production. After a 68 h irradiation, 0.04 ± 0.01 mmol H_2 was produced, corresponding to a QE (H_2) = 0.06 ± 0.03%. The system can be improved by enhancing the capacity of the semiconductors to harvest light and transfer charge, optimizing the conditions of illumination and the ratio of semiconductors with cells, among other factors. Sulfur-driven denitrification is another pathway for NO_3^- reduction, with a minor contribution. Sulfur was potentially generated from the photooxidative dissolution of CdS. However, nearly no Cd^{2+} (approximately the detection limit, 5 ppb) was detected using inductively coupled plasma mass spectrometry (ICP-MS) in supernatants after 68 h of irradiation, likely because the dissociated Cd^{2+} would be rapidly adsorbed and reprecipitated on the surface of microorganisms via biomineralization (Zhou et al., 2015). Moreover, as shown in Fig. S11 this system completely removed NO_3^--N after more than three cycles (> 5 days), which was more stable than the common CdS photocatalytic system (Spanhel et al., 1987). Moreover, *T. denitrificans*-CdS hybrids are a stable and self-healing system (Sakimoto et al., 2018). The interactions between those two mechanisms warrant further investigation to develop a more effective light-driven denitrification system.

3.5. Implications

The findings from this study have important implication for the recovery of high-energy compounds from contaminants. The efficient conversion of contaminants to high-energy compounds will benefit both the environment and energy requirements. Under irradiation, *T. denitrificans*-CdS completely removed NO_3^- and the amount of N_2O generated in the gaseous products was > 96%; this purity is much higher than the product generated by CANDO (60–70%) (Scherson et al., 2013b; Scherson et al., 2014). The high purity of N_2O is critically important for large-scale production and avoids extensive efforts in separation and purification of the products. The proposed system does not require bioavailable organic substrates, eliminating the risk of secondary organic pollution and reducing sludge production (Myung et al., 2015; Scherson et al., 2014). In addition, solar energy represents a more economic and sustainable way of producing electrons for NO_3^-

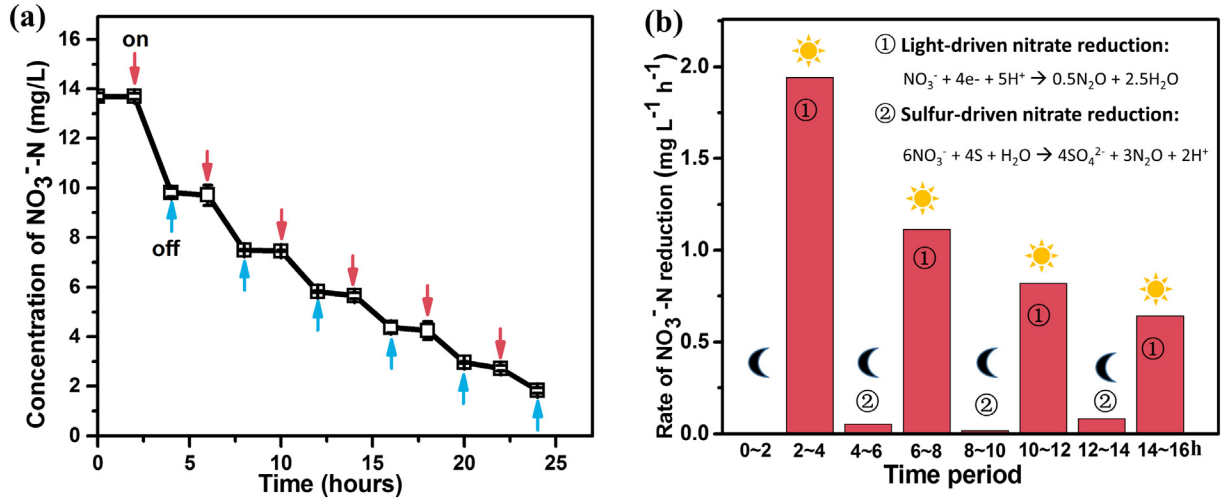

Fig. 4. Light-driven nitrate reduction by *T. denitrificans*-CdS in light off-on cycles. (a) NO_3-N reduction by *T. denitrificans*-CdS hybrids with light off-on cycles of 2 h. (b) The average rate of NO_3-N reduction (mg/L h^{-1}) in two hours' reactions.

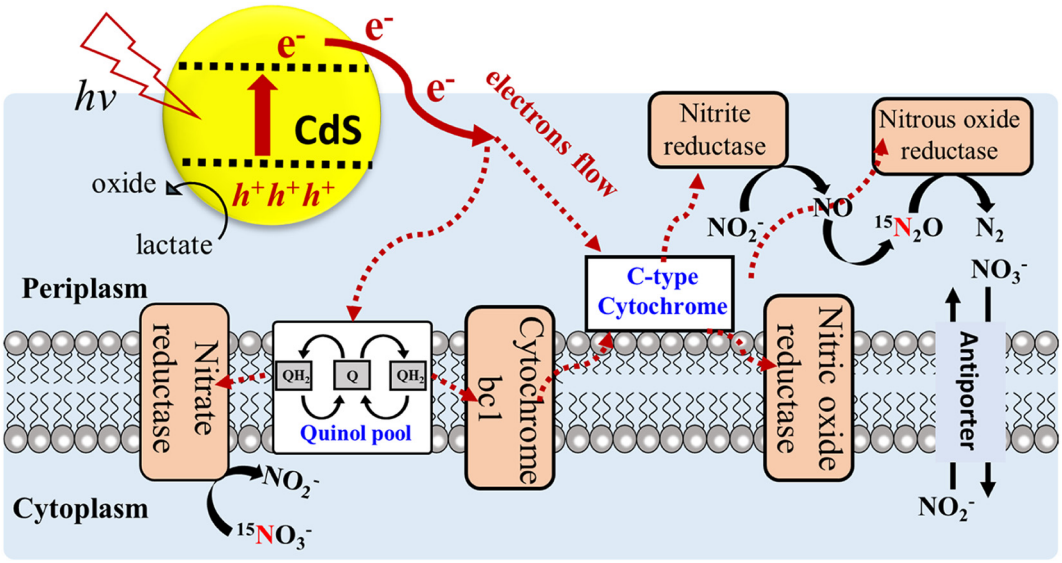

Fig. 5. Proposed mechanism of the light-driven microbial denitrification by *T. denitrificans*-CdS hybrids.

reduction than heterotrophic or conventional autotrophic denitrification (sulfur/hydrogen serving as electron donors) (Park and Yoo, 2009). This strategy could be applied to the traditional nitrogen removal process in the field of environmental engineering, such as the famous nitrification-denitrification cycle, to expand its applications. Therefore, light-driven denitrification has a potential to become a significant revolution not only in NO_3^- removal but also in N_2O production from wastewater. Moreover, because of the extensive distribution of *T. denitrificans* in both soil and water, mechanisms similar to the light-driven nonphototrophic denitrification may widely occur in a mineral-enriched environment, such as paddy soils, which contains abundant microbes, semiconductive minerals (e.g., hematite, anatase, sphalerite, etc.) and nitrate (Kato et al., 2010; Lu et al., 2012; Shi et al., 2016). Thus, this study may provide insights that will enable us to understand the elements involved in biochemical cycling, particularly in nitrogen cycling, at the interface of microbes-semiconductors. Our finding might also provide guidance in the control of the discharge of nitrogen-contaminant water into the mineral-enriched environment for the reduction of N_2O emissions.

4. Conclusions

In this study, we provide the first proof of concept evidence for sustainable and low-cost autotrophic denitrification to generate highly pure N_2O from NO_3^- in a reaction driven by light through the construction a CdS photosensitized *Thiobacillus denitrificans*. Upon irradiation, the inorganic-biological system *T. denitrificans*-CdS is capable of completely removing the NO_3^- and producing the high-value fuel gas N_2O, whose purity in gaseous products is > 96.4 ± 0.4%. The photoexcited electrons serve as the dominant electron sources for NO_3^- reduction by *T. denitrificans*-CdS. Light-driven denitrification has important implications in the removal of nitrogen from wastewater in an economic manner and recovery of energy from nitrogen.

Competing finance interest

The authors declare no competing financial interest.

Acknowledgment

This work was supported by the National Natural Science Foundation of China (21607023, 41671264 and 91751109).

Appendix A. Supplementary data

Supplementary data to this article can be found online at https://doi.org/10.1016/j.envint.2019.03.045.

References

Adouani, N., Lendormi, T., Limousy, L., Sire, O., 2010. Effect of the carbon source on N_2O emissions during biological denitrification. Resour. Conserv. Recy. 54, 299–302.
Alefounder, P.R., Ferguson, S.J., 1982. Electron transport-linked nitrous oxide synthesis and reduction by *Paracoccus denitrificans* monitored with an electrode. Biochem. Biophys. Res. Commun. 104, 1149–1155.
Beaulieu, J.J., Tank, J.L., Hamilton, S.K., Wollheim, W.M., Hall, R.O., Mulholland, P.J., Peterson, B.J., Ashkenas, L.R., Cooper, L.W., Dahm, C.N., Dodds, W.K., Grimm, N.B., Johnson, S.L., McDowell, W.H., Poole, G.C., Valett, H.M., Arango, C.P., Bernot, M.J., Burgin, A.J., Crenshaw, C.L., Helton, A.M., Johnson, L.T., O'Brien, J.M., Potter, J.D., Sheibley, R.W., Sobota, D.J., Thomas, S.M., 2011. Nitrous oxide emission from denitrification in stream and river networks. Proc. Natl. Acad. Sci. U. S. A. 108, 214–219.
Bell, L.C., Ferguson, S.J., 1991. Nitric and nitrous oxide reductases are active under aerobic conditions in cells of *Thiosphaera pantotropha*. Biochem. J. 273 (Pt 2), 423–427.
Bosch, J., Lee, K.Y., Jordan, G., Kim, K.W., Meckenstock, R.U., 2012. Anaerobic, nitrate-dependent oxidation of pyrite nanoparticles by *Thiobacillus denitrificans*. Environ. Sci. Technol. 46, 2095–2101.
Chaturvedi, S., Dave, P.N., 2013. Review on thermal decomposition of ammonium nitrate. J. Energ. Mater. 31, 1–26.
Chen, J., Strous, M., 2013. Denitrification and aerobic respiration, hybrid electron transport chains and co-evolution. BBA-Bioenergetics 1827, 136–144.
Coyle, C.L., Zumft, W.G., Kroneck, P.M., Korner, H., Jakob, W., 1985. Nitrous oxide reductase from denitrifying *Pseudomonas perfectomarina*. Purification and properties of a novel multicopper enzyme. Eur. J. Biochem. 153, 459–467.
Ghafari, S., Hasan, M., Aroua, M.K., 2008. Bio-electrochemical removal of nitrate from water and wastewater - a review. Bioresour. Technol. 99, 3965–3974.
Harada, H., Sakata, T., Ueda, T., 1985. Effect of semiconductor on photocatalytic decomposition of lactic acid. J. Am. Chem. Soc. 107, 1773–1774.
Jiang, Z., Wang, B., Yu, J.C., Wang, J., An, T., Zhao, H., Li, H., Yuan, S., Wong, P.K., 2018. $AgInS_2/In_2S_3$ heterostructure sensitization of *Escherichia coli* for sustainable hydrogen production. Nano Energy 46, 234–240.
Kampschreur, M.J., Temmink, H., Kleerebezem, R., Jetten, M.S.M., van Loosdrecht, M.C.M., 2009. Nitrous oxide emission during wastewater treatment. Water Res. 43, 4093–4103.
Kato, S., Nakamura, R., Kai, F., Watanabe, K., Hashimoto, K., 2010. Respiratory interactions of soil bacteria with (semi)conductive iron-oxide minerals. Environ. Microbiol. 12, 3114–3123.
Kelly, P.T., He, Z., 2014. Nutrients removal and recovery in bioelectrochemical systems: a review. Bioresour. Technol. 153, 351–360.
Kornienko, N., Sakimoto, K.K., Herlihy, D.M., Nguyen, S.C., Alivisatos, A.P., Harris, C.B., Schwartzberg, A., Yang, P., 2016. Spectroscopic elucidation of energy transfer in hybrid inorganic-biological organisms for solar-to-chemical production. Proc. Natl. Acad. Sci. U. S. A. 113, 11750–11755.
Larkum, A.W.D., 2010. Limitations and prospects of natural photosynthesis for bioenergy production. Curr. Opin. Biotechnol. 21, 271–276.
Law, Y., Ye, L., Pan, Y., Yuan, Z., 2012. Nitrous oxide emissions from wastewater

treatment processes. Philos. T. Roy. Soc. 367, 1265.
Lee, K.C., Rittmann, B.E., 2002. Applying a novel autohydrogenotrophic hollow-fiber membrane biofilm reactor for denitrification of drinking water. Water Res. 36, 2040–2052.
Lu, A., Li, Y., Jin, S., Wang, X., Wu, X.L., Zeng, C., Li, Y., Ding, H., Hao, R., Lv, M., 2012. Growth of non-phototrophic microorganisms using solar energy through mineral photocatalysis. Nat. Commun. 3, 768.
Molstad, L., Dörsch, P., Bakken, L.R., 2007. Robotized incubation system for monitoring gases (O_2, NO, N_2O N_2) in denitrifying cultures. J. Microbiol Meth. 71, 202–211.
Myung, J., Wang, Z., Yuan, T., Zhang, P., Nostrand, J.D.V., Zhou, J., Criddle, C.S., 2015. Production of nitrous oxide from nitrite in stable type II methanotrophic enrichments. Environ. Sci. Technol. 49, 10969–10975.
Pan, Y., Ye, L., Yuan, Z., 2013. Effect of H_2S on N_2O reduction and accumulation during denitrification by methanol utilizing denitrifiers. Environ. Sci. Technol. 47, 8408–8415.
Park, J.Y., Yoo, Y.J., 2009. Biological nitrate removal in industrial wastewater treatment: which electron donor we can choose. Appl. Microbiol. Biotechnol. 82, 415–429.
Richardson, D., Felgate, H., Watmough, N., Thomson, A., Baggs, E., 2009. Mitigating release of the potent greenhouse gas N2O from the nitrogen cycle – could enzymic regulation hold the key? Trends Biotechnol. 27, 388–397.
Sakimoto, K.K., Wong, A.B., Yang, P., 2016. Self-photosensitization of nonphotosynthetic bacteria for solar-to-chemical production. Science 351, 74.
Sakimoto, K.K., Kornienko, N., Cestellos-Blanco, S., Lim, J., Liu, C., Yang, P.D., 2018. Physical biology of the materials-microorganism interface. J. Am. Chem. Soc. 140, 1978–1985.
Santin, I., Barbu, M., Pedret, C., Vilanova, R., 2017. Control strategies for nitrous oxide emissions reduction on wastewater treatment plants operation. Water Res. 125, 466–477.
Scherson, Y., Lohner, K., Lariviere, B., Cantwell, B., Kenny, T., 2013a. A monopropellant gas generator based on N_2O decomposition for “Green” propulsion and power generation. In: AIAA/ASME/SAE/ASEE Joint Propulsion Conference & Exhibit.
Scherson, Y.D., Wells, G.F., Woo, S.G., Lee, J., Park, J., Cantwell, B.J., Criddle, C.S., 2013b. Nitrogen removal with energy recovery through N_2O decomposition. Energy Environ. Sci. 6, 241–248.
Scherson, Y.D., Woo, S.G., Criddle, C.S., 2014. Production of nitrous oxide from anaerobic digester centrate and its use as a co-oxidant of biogas to enhance energy recovery. Environ. Sci. Technol. 48, 5612–5619.
Shao, M.-F., Zhang, T., Fang, H.H.-P., 2010. Sulfur-driven autotrophic denitrification: diversity, biochemistry, and engineering applications. Appl. Microbiol. Biotechnol. 88, 1027–1042.
Shi, L., Dong, H., Reguera, G., Beyenal, H., Lu, A., Liu, J., Yu, H.-Q., Fredrickson, J.K., 2016. Extracellular electron transfer mechanisms between microorganisms and minerals. Nat. Rev. Microbiol. 14, 651.
Spanhel, L., Haase, M., Weller, H., Henglein, A., 1987. Photochemistry of colloidal semiconductors. 20. Surface modification and stability of strong luminescing CdS particles. J. Am. Chem. Soc. 109, 5649–5655.
Thauer, R.K., Jungermann, K., Decker, K., 1977. Energy conservation in chemotrophic anaerobic bacteria. Bacteriol. Rev. 41, 100–180.
Van Doan, T., Lee, T.K., Shukla, S.K., Tiedje, J.M., Park, J., 2013. Increased nitrous oxide accumulation by bioelectrochemical denitrification under autotrophic conditions: kinetics and expression of denitrification pathway genes. Water Res. 47, 7087–7097.
Wang, B., Zeng, C., Chu, K.H., Wu, D., Yip, H.Y., Ye, L., Wong, P.K., 2017. Enhanced biological hydrogen production from Escherichia coli with surface precipitated cadmium sulfide nanoparticles. Adv. Energy Mater. 7, 1700611.
Wei, W., Sun, P., Li, Z., Song, K., Su, W., Wang, B., Liu, Y., Zhao, J., 2018. A surface-display biohybrid approach to light-driven hydrogen production in air. Sci. Adv. 4, 9253.
Wei-Kang, W., Jie-Jie, C., Wen-Wei, L., Dan-Ni, P., Xing, Z., Han-Qing, Y., 2015. Synthesis of Pt-loaded self-interspersed anatase TiO_2 with a large fraction of (001) facets for efficient photocatalytic nitrobenzene degradation. Acs Appl. Mater. Inter. 7, 20349–20359.
Xu, L., Zhao, Y., Owusu, K.A., Zhuang, Z., Liu, Q., Wang, Z., Li, Z., Mai, L., 2018. Recent advances in nanowire-biosystem interfaces: from chemical conversion, energy production to electrophysiology. Chem. 4, 1538–1559.
Yu, L., Yuan, Y., Chen, S., Zhuang, L., Zhou, S., 2015. Direct uptake of electrode electrons for autotrophic denitrification by *Thiobacillus denitrificans*. Electrochem. Commun. 60, 126–130.
Zhang, T.C., Lampe, D.G., 2015. Sulfur:limestone autotrophic denitrification processes for treatment of nitrate-contaminated water: batch experiments. Water Res. 33, 599–608.
Zhang, W., Wang, Y., Wang, Z., Zhong, Z., Xu, R., 2010. Highly efficient and noble metal-free NiS/CdS photocatalysts for H2 evolution from lactic acid sacrificial solution under visible light. Chem. Commun. 46, 7631–7633.
Zhang, H., Liu, H., Tian, Z., Lu, D., Yu, Y., Cestellos-Blanco, S., Sakimoto, K.K., Yang, P., 2018. Bacteria photosensitized by intracellular gold nanoclusters for solar fuel production. Nat. Nanotechnol. 13, 900–905.
Zhou, J., Yang, Y., Zhang, C.-y., 2015. Toward biocompatible semiconductor quantum dots: from biosynthesis and bioconjugation to biomedical application. Chem. Rev. 115, 11669–11717.
Zhu, N., Wu, Y., Tang, J., Duan, P., Yao, L., Rene, E.R., Wong, P.K., An, T., Dionysiou, D.D., 2018. A new concept of promoting nitrate reduction in surface waters: simultaneous supplement of denitrifiers, electron donor pool, and electron mediators. Environ. Sci. Technol. 52, 8617–8626.